This is the accepted manuscript of the article, which has been published online ahead of print, 2020 Aug 9, in *Current Cardiology Reviews*. The final published version is available at EurekaSelect via http://dx.doi.org/10.2174/1573403X16666200810105504.

The vectorcardiogram and the main dromotropic disturbances

Andrés Ricardo **Pérez-Riera,** MD PhD[1]; Raimundo **Barbosa-Barros,** MD[2]; Rodrigo **Daminello-Raimundo,** PhD[1]; Luiz Carlos **de Abreu,** PhD[1,3]; Kjell **Nikus,** MD PhD[4]

[1]Laboratório de Metodologia de Pesquisa e Escrita Científica, Faculdade de Medicina do ABC, Santo André, São Paulo, Brazil.

[2]Coronary Center of the Hospital de Messejana Dr. Carlos Alberto Studart Gomes, Fortaleza, Ceará, Brazil.

[3]Graduate Entry Medical School, University of Limerick, Limerick, Ireland.

[4]Heart Center, Tampere University Hospital and Faculty of Medicine and Health Technology, Tampere University, Finland.

Introduction

The vectorcardiogram (VCG) is the spatial representation of electromotive forces generated during cardiac activity analyzed in three spatial planes. Consequently, the method provides three-dimensional information of the electric activity of the atria and the ventricles. VCG has advantages over the electrocardiogram (ECG); the spatial orientation and the magnitude of the vectors give a better idea of the magnitude and direction of electrical forces at any moment. Additionally, the VCG is still superior to the ECG in specific situations, such as to differentiate left anterior fascicular block (LAFB) from inferior myocardial infraction (MI) with left axis deviation [1], which is important for more accurate diagnosis of chamber enlargement and fascicular blocks associated with MI. LAFB is always accompanied by counterclockwise (CCW) inscription of the QRS loop whereas inferior MI invariably has clockwise (CW) inscription of the loop. Studies have shown the VCG to be more sensitive to the diagnosis and localization of infarction than the ECG [2]. When properly utilized, VCG should remain a valuable diagnostic as well as teaching tool [3]. VCG has greater specificity and sensitivity related to ECG for the diagnosis of chamber enlargement, fascicular blocks, and ventricular pre-excitation in association with MI. It is useful in diagnosing the coexistence of fascicular blocks and inferior MI. ECG criteria for the diagnosis of inferior wall MI are highly specific, but insensitive compared with VCG criteria [4]. In the fields of education and research, VCG provides a better insight into the electrical phenomena that occur spatially, and has important impact on the progress of electrocardiographic science. We hope that the use of this resource will not get lost over time, since VCG still represents a source to enrich science by enabling a better morphological interpretation of the electrical phenomena.

In the present review, we will analyze the VCG characteristics of atrial and ventricular conduction disorders such as complete interatrial block (IAB), left and right bundle branch block (RBBB), left fascicular blocks and ventricular preexcitation.

1. Complete, advanced or third-degree IAB

In these cases, the stimulus is blocked in the Bachmann bundle (BB) region, and the left atrium (LA) is retrogradely activated with a P wave duration ≥120 ms and plus-minus (+/-) P wave in the inferior leads II, III and aVF. There is an open angle ≥90° between the vector of the first and second part of the P wave in the inferior leads. Orthogonal Y lead plus-minus with a negative mode >40 ms appear with notches and slurs in the last part of the P loop. IAB is often associated with left atrial enlargement (LAE) (up to 90% of cases) and dysfunction, decreased left ventricular (LV) filling [5], propensity for LA appendage thrombosis, increased atrial natriuretic peptide levels, and is a predictor of paroxysmal supraventricular tachyarrhythmias such as atrial fibrillation (AF), atrial flutter as well as an exacerbation of LV failure [6]. The prevalence of first degree IAB(P wave of 120 milliseconds or more, usually bimodal, is especially visible in leads I, II, or III, and (b) the P wave morphology in V1 in the absence of left atrial enlargement (LAE) presents a P wave negative mode that is less evident than in cases of LAE, because in the absence of LAE, the P loop is directed in a less backward direction) is much higher than complete IAB. The ECG pattern of complete IAB is an extremely strong marker of supraventricular tachyarrhythmia much more so than the presence of first degree or partial IAB. Bayés de Luna A et al. [7] studied 16 patients with ECG evidence of complete IAB, eight patients with valvular heart disease, four with dilated cardiomyopathy and four with other forms of heart disease. Patients with valvular heart disease and cardiomyopathy were compared with a control group of 22 patients with similar clinical and

echocardiographic characteristics, but without this type of IAB. Patients with complete IAB (ECG signs of retrograde activation of the LA) had a much higher incidence of paroxysmal supraventricular tachyarrhythmias during follow-up than did the control group. Eleven of 16 patients with complete IAB had atrial flutter (atypical in seven cases, typical in two cases, and with two or more morphologies in two cases). Six patients from the control group had sustained atrial tachyarrhythmias (five AF and one typical atrial flutter). Evidently, the atrial tachyarrhythmias were due more to advanced IAB and retrograde activation of LA and frequent premature atrial contractions (PACs) than to LAE, because the control group with a LA of the same size, but without complete IAB and retrograde activation of LA and with less incidence of PACs, had a much lower incidence of paroxysmal tachycardia.

Bayés de Luna et al. [8] demonstrated the value of preventive antiarrhythmic treatment in patients with complete IAB. In this population LAE is present in 90% of cases.

From 81,000 ECGs, Bayes de Luna et al [9] collected 83 cases that fulfilled the criteria of Interatrial Conduction Disturbances with Left Atrial Retrograde Activation (IACD-LARA) (P +/- in II, III and VF with P width ≥120 ms); this is equivalent to complete IAB. The authors presented a detailed study of 35 cases with surface ECG/VCG and 29 cases with orthogonal ECG leads. Two control groups were included: one with (30 cases) and one without known heart disease (25 cases). The prevalence of IACD-LARA was nearly 1% in the whole study population and 2% among patients with valvular heart disease. Arrhythmias, such as AF and atrial flutter, were observed in >90% of the patients with complete IAB.

Diagnosis criteria of complete IAB and retrograde activation of the LA [7, 10-12]:

- biphasic, bifid, or notched “plus-minus” P waves in the inferior leads II, III and aVF of the ECG and Y orthogonal lead of VCG

- ECG: P-wave duration ≥120 ms
- VCG: angle between the first portion (RA) and end portion (LA) >90º
- VCG: orthogonal Y lead plus-minus with the final negative portion ≥40 ms
- ≥40 ms final portion of the P loop is located below the X and Z leads orthogonal X and Z leads
- VCG: delayed final portion of the P loop, notches and slurring in the last part of the P loop
- high esophageal lead recording: positive P wave polarity and P-wave delay
- low esophageal lead recording: plus-minus P wave polarity and P-wave delay
- intracavitary ECG recording: P wave craniocaudal activation inside the RA
- intracavitary ECG recording: P wave caudal-cranial activation inside LA.

Complete IAB should be considered as the ECG/VCG manifestation of the Bayés' Syndrome [13] (Figure 1).

Figure 1

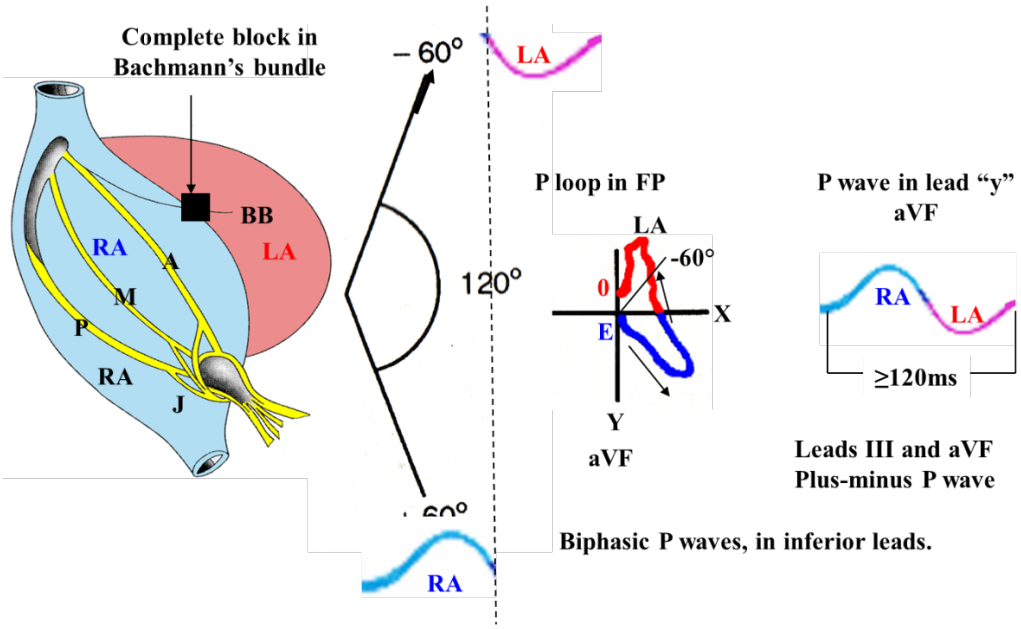

The electrical impulse is blocked/delayed in the BB region, but retrograde left atrial activation usually occurs [14]. Note the existence of an open angle between the vector

of the first (RA) and the last (LA) portion of the P wave. Retrograde activation of the LA has been demonstrated in electrophysiological studies [15]. Consequently, P loop/wave in the orthogonal lead "Y", aVF and III is biphasic plus-minus. LA activation occurs by an alternate route rather than proceeding from right to left via the BB [16].

2. VCG features of complete right bundle branch block

The VCG of complete RBBB (CRBBB) takes into account only the QRS loop in the horizontal plane (HP). There are three recognized VCG patterns: Grishman or Kennedy type I, Cabrera or Kennedy type II, and Kennedy type III or C (Figure 2).

Figure 2

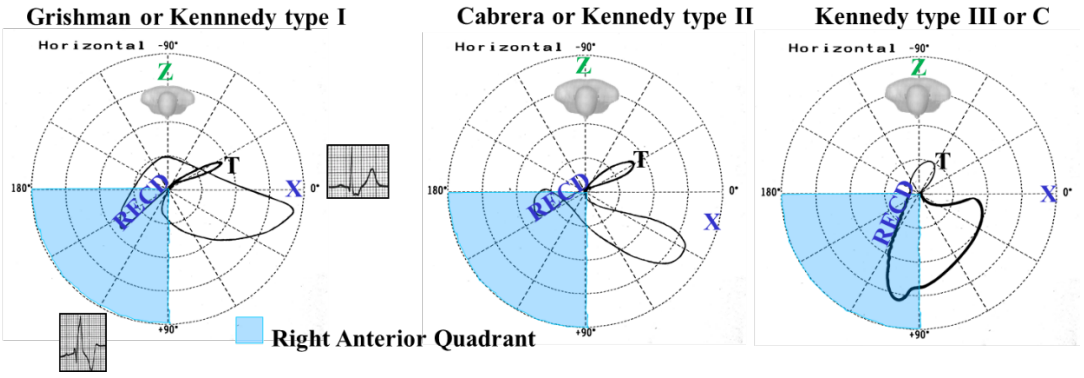

In the three patterns, the terminal vector of 60 to 120ms or more have "glove finger" shape (finger-like terminal appendix) located in the right anterior quadrant in the HP. The Cabrera or Kennedy type II pattern is frequently associated with moderate right ventricular hypertrophy (RVH), and Kennedy type III or C with severe RVH [17].

Possible etiologies of complete right bundle branch block

Normal variant: the incidence is 1.8 per 1.000. Below age 30 the incidence is 1.3 per 1.000 and between ages 30 and 44 it ranged from 2.0 to 2.9 per 1,000 (Hiss 1962), RBBB and incomplete RBBB (IRBBB) were two to three times more common among men than

women. RBBB was associated with increased cardiovascular risk and all-cause mortality, whereas IRBBB was not. Contrary to common perception, RBBB in asymptomatic individuals should alert clinicians to consider increased risk for cardiovascular events [18].

Congenital Heart Diseases. Associated disease are**:** atrial septal defects (in more than 90% of cases), both the ostium secundum and the ostium primum type [19]; partial or total anomalous pulmonary vein drainage to the right atrium; Ebstein's anomaly [20]; Uhl's anomaly [21]; ventricular septal defects (VSDs) in the presence of biventricular hypertrophy; pulmonary stenosis, especially in the moderate form and particularly in pulmonary stenosis of tetralogy of Fallot (ToF) or large VSD [22]; ToF (pre- and post-surgery) [23]; aortic stenosis: congenital, bivalvular, degenerative; after alcohol injection into the first septal perforator branch of the left anterior descending (LAD) coronary artery in hypertrophic obstructive cardiomyopathy [24].

Genetic-familial causes: Brugada syndrome: atypical CRBBB, frequently with absence of wide S wave in the left precordial leads and ST segment elevation from V1 to V3 (SCN5A gene). Additionally, Brugada syndrome can be masked by CRBBB [25].

3. RBBB associated with left anterior fascicular block

The initial portion of the loop behaves as a left anterior fascicular block (LAFB) and the final part as a CRBBB. The duration of the QRS loop ≥120 ms.

Frontal plane (FP): very similar to isolated LAFB loop: initial vectors from 10 to 20ms heading downward and to the right (type I) or downward and to the left (type II); QRS loop of CCW rotation; QRS axis in the frontal plane (SÂQRS) with extreme deviation to the left beyond -30°; efferent branch of the QRS loop heading to the left and finally to the

left and upward; afferent branch that begins above and slightly to the left, to finally end in a final appendage of slow recording and located to the right and above.

HP: typical QRS loop of a CRBBB [26]; vectors from initial 10 to 20 ms heading to the front and the right or left [27]; efferent branch of QRS loop from right to left and with variable degrees of anteriorization; main body of QRS loop with CCW (type I), eight or CW rotation (type II). The type of rotation seems to lack clinical significance; however, type II appears in a greater number of patients in chronic heart failure; the afferent branch of the QRS loop in front of the X line from left to right; the efferent branch of the QRS loop behind or in front of the X line; end delay located in the right anterior quadrant [28, 29]; ventricular repolarization with the T loop opposite to the final portion of the QRS loop to the left, behind and below [30] (Figure 3).

Figure 3

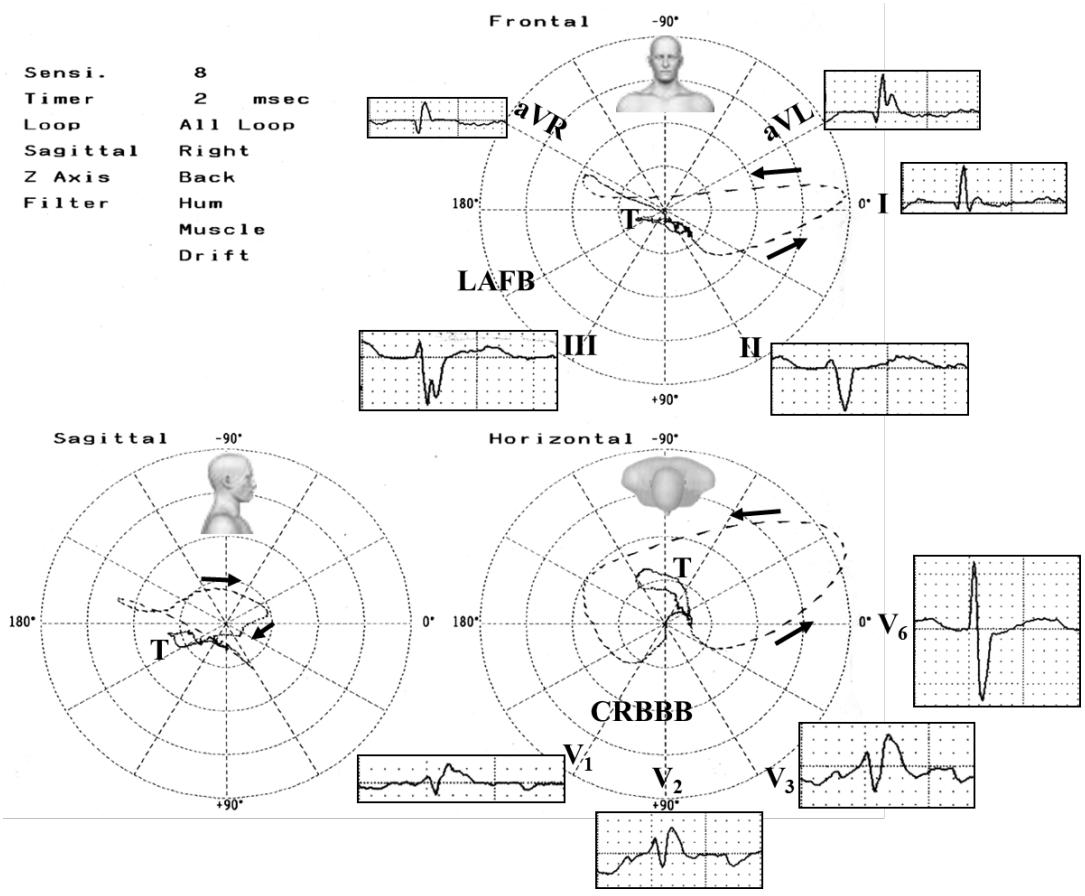

Clinical diagnosis: Chronic chagasic myocarditis.

VCG: Extreme left axis deviation as a consequence of LAFB associated with CRBBB Grishman type observed in the HP. LAFB+RBBB is a typical pattern of chronic chagasic myocarditis.

LAFB+RBBB constitutes the most frequent type of bifascicular block. In the developed countries, the prevalence in the general population is ~1.4%.

LAFB+RBBB is the hallmark of chronic chagasic myocarditis, which constitutes the most frequent association in Latin America, where it exists from the Argentinean Patagonia up to the frontier with USA. In CRBBB of chronic chagasic myocarditis, a strong association (70% prevalence) with LAFB stands out. In patients younger than 40 years, from the endemic area, with CRBBB + LAFB, there is a high suspicion of chronic chagasic myocarditis, and even more with the additional presence of polymorphic ventricular extrasystoles and primary alterations of ventricular repolarization. The most frequent ECG pattern is typical (His bundle) CRBBB and LAFB. A longitudinal study of 5,710 infected patients showed that the presence of CRBBB associated to primary alterations of repolarization and electrically inactive areas indicates high risk of death. Autopsy studies conducted by Andrade, revealed that most of the patients with chronic chagasic heart disease present a significant involvement of the conduction system at the level of the nodal-His bundle (N-H) region of the AV node, the right penetrating and branching portion of the His bundle, proximal portion of the right bundle branch (RBB) and the left anterior fascicle (LAF) of the left branch. CRBBB of chronic chagasic heart disease is of the proximal type [31]. The most common ECG changes are the following: CRBBB (35%) and LAFB (35%). RBBB with LAFB is strongly related to Chagas disease in older patients [32].

Other etiologies of LAFB + RBBB

The prevalence of LAFB + RBBB in coronary heart disease (CHD), which represents the main cause in the developed countries, was is ~1% in the hospital population. Post-myocardial infarction (MI), the prevalence is ~6%, almost always caused by obstruction of the LAD, since the RBB and the LAF are irrigated by the perforator branches of this artery. Other etiologies are: hypertensive heart disease (in 20 to 25%); sclerodegenerative disease of the His system, genetic Lenègre disease with or without high blood pressure; Lev disease or sclerosis of the left side of the cardiac skeleton; and chest trauma. Closed trauma of the chest is frequently accompanied by CRBBB. In this case, the CRBBB frequently disappears after some hours. LAFB and RBBB may also be appear in a familial form with syncope or sudden death, or it may be congenital and isolated. It may be associated with non-chagsic myocarditis; sarcoidosis; granulomatosis; aortic valve disease; hyperkalemia or hyperpotassemia; progressive external ophthalmoplegia. Post-surgery this bifascicular block may be seen:

1) After corrective surgery of ToF (7 to 25% of the cases). It is of truncal type and indicates that the LAF has been injured during patch suturation to increase size of the right ventricular outflow tract. The patients that remain with bifascicular block after corrective surgery do not have higher late mortality risk.

2) In 4% of patients after corrective surgery of VSD.

3) After tricuspid valve surgery.

4) After bypass surgery with internal thoracic arterial and/or saphenous vein grafts (4%). CRBBB in isolation was observed in 6% and LAFB in 6%.

4. VCG in compete left bundle branch block (CLBBB)

The VCG diagnosis is made by using the HP (Figure 4).

Figure 4

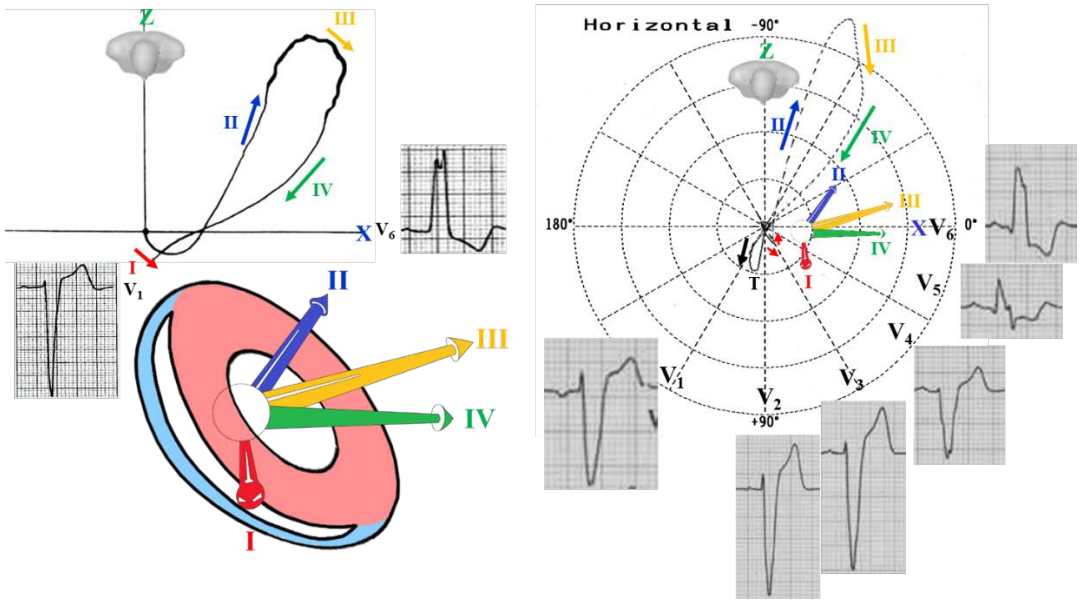

VCG criteria in the HP

Narrow, long QRS loop, and with morphology usually in “eight”; the QRS loop duration is ≥120 ms; the QRS loop shape is elongated and narrow; the main body of the QRS loop is inscribed posteriorly and to the left within the range of - 90 to - 40°; maximal vector of QRS located in the left posterior quadrant (between –40º to -80º) and of increased magnitude (>2 mV); the main portions of the QRS loop of CW rotation. CCW rotation may indicate parietal CLBBB or association with lateral infarction or severe left ventricular hypertrophy (LVH); the efferent limb (II) located to the right related to the afferent limb (III and IV); conduction delay noted in the mid and terminal portion; the main body of QRS loop is inscribed CW; the magnitude of the max QRS vector is increased above normal exceeding 2mV; the ST segment and T wave vector are directed rightward and anteriorly; the T loop of CCW recording. The CW rotation of T wave in this plane suggests CLBBB complicated with infarction or LVH [33].

Possible etiologies of CLBBB: systemic hypertension (SH) [34]; CHD [35]; association of SH and CHD; cardiomyopathies: in idiopathic dilated cardiomyopathy CLBBB is observed in ≈25% of cases [36] [37]; diffuse myocardial disease; myocarditis; aortic valve disease [38]; mitral valve disease [39]; sclerosis of the left side of the cardiac skeleton: Lev disease [40]; familial progressive cardiac conduction defect (PCCD), "idiopathic" sclerosis of the His conduction system or Lenègre disease. Several genes, such as SCN5A [41], SCN1B and TRPM4, may be involved and result in familial PCCD [42]. It is usually inherited in an autosomal dominant manner also autosomal recessive inheritance and sporadic cases have been reported. Rare LBBB etiologies are: cardiomyopathies associated with collagenous disease [43]; congenital heart diseases (late phase of aortic stenosis); blood or crystalloid cardioplegia; use of taxol, cytotoxic antineoplastic drugs [44]; primary amyloidosis [45]; sarcoidosis [46]; hyperpotassemia [47]; postoperatively in hypertrophic obstructive cardiomyopathy [24]; after coronary angiography [48]; without apparent cause (idiopathic, cryptogenetic, primary or essential).

5. VCG characteristics of fascicular blocks: left anterior, posterior, and septal fascicular block

LAFB and left posterior block are mainly diagnosed by alterations in the FP. In contrast, LSFB affects only the HP (Figure 5).

Figure 5

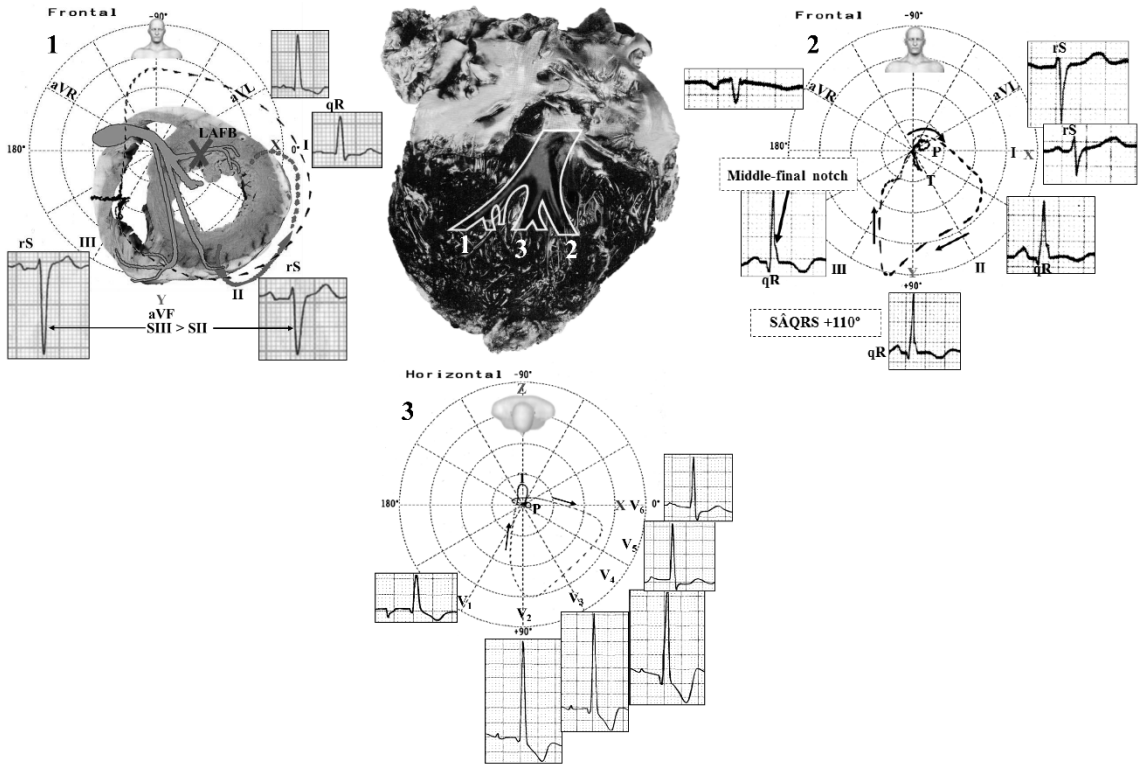

LAFB (1): VCG in the FP: QRS loop ≤ 100 ms. When intermittent, the increase does not exceed 20 ms; constant CCW rotation of QRS loop when not associated with other diseases; in the presence of LVH or anterior MI, the rotation of the initial 20 ms may change; vector of initial 10 to 20 ms heading inferiorly; maximal vector of QRS heading superiorly around -20º; QRS loop located in the left superior quadrant; ST/T loop always normal in non-complicated LAFB.

LPFB (2): VCG in the FP: Vector of initial 10 to 20 ms heading superiorly and to the left (near -45°) with possible delay (initial 10 to 25 ms). When associated with inferior MI, superior initial forces of ≥25 ms (more than 12.5 dashes above the orthogonal X lead. 1 dash = 2 ms) [49]; broad QRS loop, with CW rotation. According to Cooksey, Dunn and Massie, it may occasionally be in "eight" with a CCW terminal portion (10%); maximal vector near +110º (+80º to +140º); almost all the loop is located below the X

line (0 to ±180°) in inferior quadrants; 20% of the loop located in the right inferior quadrant. If there is association with CRBBB, 40% or more; afferent limb heading below and slightly to the left, and the efferent one to the right; middle-terminal portion of the QRS loop (vector of 60 ms to 100 ms) with delay. It may possibly reach the right superior quadrant; QRS loop duration up to 110 ms if in isolation. In association with CRBBB, >120 ms; normal ST-T vectors in isolated LPFB: T loop with CW rotation, heading inferiorly and to the left. If in association with CRBBB: alteration secondary to ventricular repolarization.

LPFB in the HP: QRS loop very similar to RVH of type C; QRS loop of CCW rotation. The rotation can be in "eight"; vector of initial 10 to 20 ms heading to the front and the right or left; greater area of QRS loop located in the left posterior quadrant; maximal vector of QRS around -60° to -110°; final portions with delay (60 ms to 100 ms) and located in the right posterior quadrant; 20% or more of the area of the QRS loop located in the right posterior quadrant; and T loop to the front and the left (+60°) and CW rotation.

LSFB (3): The ECG/VCG modifications are observed only in the HP/precordial leads [50]. QRS loop in the HP with an area predominantly located in the left anterior quadrant ($\geq {}^{2}/_{3}$ of the loop is facing the orthogonal X lead: 0º to ±180º); absence of normal convexity to the right of the initial 20 ms of the QRS loop; discrete dextro or rightward-orientation with moderate delay of the vector from 20 to 30 ms; anterior location of the 40 to 50 ms vector; posterior location with a reduced magnitude of the vector from 60 to 70 ms; maximal vector of the QRS loop located to the right of +30º; intermittent anterior displacement of the QRS loop; The QRS loop rotation may be CCW (incomplete LSFB) or CW: in advanced or complete LSFB or in association with CRBBB, the T loop has a tendency to posterior orientation (useful for the differential diagnosis with lateral MI).

6. **VCG in ventricular preexcitation**

The VCG findings in ventricular pre-excitation are is characterized by QRS loop conduction delay during the initial period of depolarization or slowing of inscription in the initial part of the QRS loop. In other words, there is initial slurring of the QRS complex due to the spread of activation form atria to ventricles via an accessory pathway (AP). This portion is called delta (δ) vector. When the AP has posterior location (formerly named Wolff-Parkinson-White [WPW] type A), the vector is directed anteriorly between 0° and +90°, but occasionally to the right of +90°. The maximal QRS vector is directed to the left and anteriorly in the majority of cases. In about 25% of cases, the maximal QRS vector is directed posteriorly in the HP. This subgroup may have LVH in addition to pre-excitation.

In the HP, the initial deflection is directed anteriorly and usually to the left, although occasionally to the right. The efferent limb proceeds to the left and relatively far anteriorly and then the loop turns in a CCW direction, the afferent limb passing behind the efferent limb to return on the right and anteriorly. Occasionally the entire HP QRS loop is inscribed in the CW direction and lies anteriorly and to the left. The maximal mean instantaneous vector of the HP QRS loop ranges in orientation between +20° and +95° in the majority of cases. In approximately 25% of patients, the maximal QRS vector is posteriorly located between -65° and 0°.

The frontal QRS loop tends to vary widely in configuration, although figure-eight loops are relatively common. Occasionally the frontal QRS loop has almost linear configuration. The maximal mean instantaneous vector of the frontal QRS loop is usually located between -30° and +100°. The initial deflection or δ vector may be superiorly or inferiorly directed. A superiorly oriented force will simulate an inferior MI if the initial conduction delay is not appreciated (Figure 6).

Figure 6 Example of ventricular the pre-excitation pattern with a posterior accessory pathway

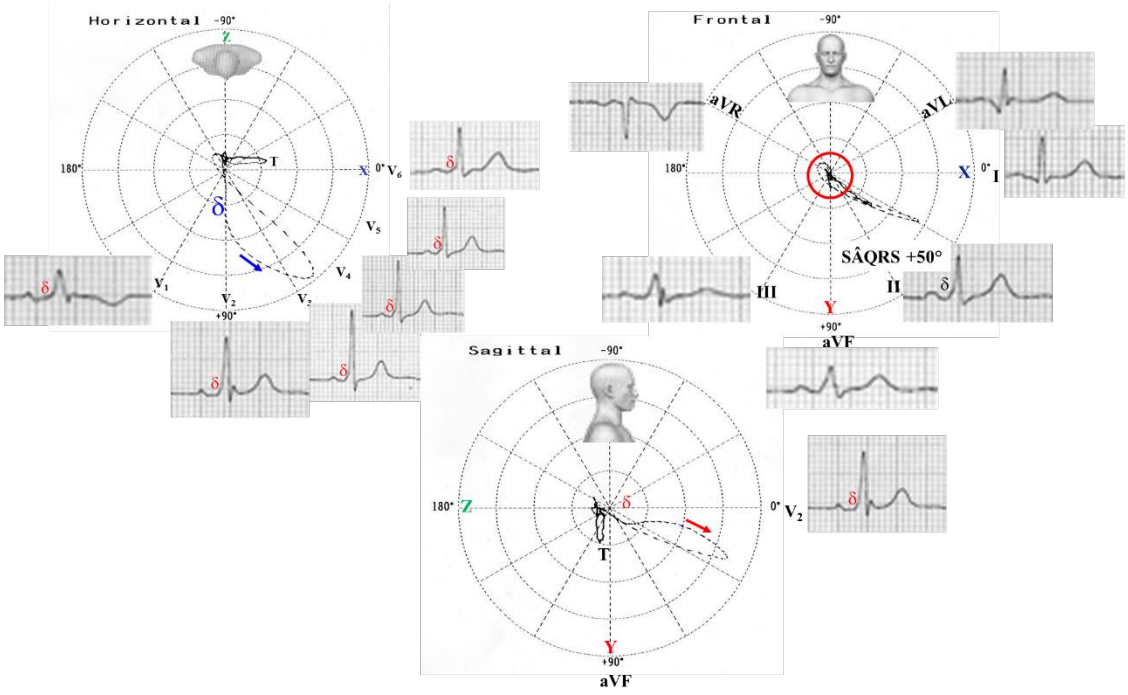

The records are quite characteristic of the ventricular pre-excitation pattern with posterior AP (previously named type A ventricular pre-excitation). The δ vector is directed anteriorly and the QRS loop is located almost entirely in the anterior left quadrant. The T loop is oriented to the left and downward.

On the other hand, when the AP is located anteriorly (previously named type B WPW), the initial δ deflection in the HP is usually directed posteriorly. The characteristic conduction delay and irregular inscription are evident in the early part of the QRS loop and each projection. Generally, the efferent limb of the QRS loop is directed to the left and posteriorly. The loop then turns in the CCW direction more posteriorly and to the left, and it remains in this quadrant until the inscription is completed. The maximal instantaneous vector of the HP QRS loop lies between 0° and -90°.

In the FP, the δ vector and the remaining QRS loop are oriented to the left, either superiorly or inferiorly. The QRS loop may be inscribed in CW, CCW or in figure-eight configuration. The maximal mean instantaneous vector of the frontal loop is generally situated between -45° and -30°.

Ebstein's anomaly is associated with the WPW syndrome (type B according to the old nomenclature) in 5 to 25% of cases (previously called type B), and it may be associated with left axis deviation. Ebstein's anomaly is the congenital heart disease most frequently associated with WPW.

Patients with left-sided APs rarely show organic heart disease, while in 45% of the right-sided Aps, there is an association to organic heart disease [51]. The locations of the AP in Ebstein's anomaly are: right anterior (the most frequent one), right lateral, right posterior and right posteroseptal.

There are rare cases of Ebstein's anomaly with pre-excitation of the Mahaim type: normal PR interval with δ wave that resembles CLBBB. Ebstein's anomaly with CLBBB may correspond to the Mahaim type of pre-excitation. Mahaim pre-excitation is due to fibers that involve the His-nodal system, either from the AV node, or from the His bundle or its branches, expressed as two variants: ventricular nodal (connections) and fasciculoventricular (tracts).

References

1. Benchimol A, Desser KB, Schumacher J. Value of the vectorcardiogram for distinguishing left anterior hemiblock from inferior infarction with left axis deviation. Chest. 1972;61:74-6. doi: 10.1378/chest.61.1.74]

2. Lee GB, Wilson WJ, Amplatz K, *et al.* Correlation of vectorcardiogram and electrocardiogram with coronary arteriogram. Circulation. 1968;38:189-200. doi: 10.1161/01.cir.38.1.189]

3. Chou TC. When is the vectorcardiogram superior to the scalar electrocardiogram? J Am Coll Cardiol. 1986;8:791-9. doi: 10.1016/s0735-1097(86)80419-3]

4. Hurd HP, 2nd, Starling MR, Crawford MH, *et al.* Comparative accuracy of electrocardiographic and vectorcardiographic criteria for inferior myocardial infarction. Circulation. 1981;63:1025-9. doi: 10.1161/01.cir.63.5.1025]

5. de Luna AB, Masso-van Roessel A, Robledo LAE. The Diagnosis and Clinical Implications of Interatrial Block. Eur Cardiol. 2015;10:54-9. [PMID: 6159419 doi: 10.15420/ecr.2015.10.01.54]

6. Escobar-Robledo LA, Bayes-de-Luna A, Lupon J, *et al.* Advanced interatrial block predicts new-onset atrial fibrillation and ischemic stroke in patients with heart failure: The "Bayes' Syndrome-HF" study. Int J Cardiol. 2018;271:174-80. doi: 10.1016/j.ijcard.2018.05.050]

7. Bayes de Luna A, Cladellas M, Oter R, *et al.* Interatrial conduction block and retrograde activation of the left atrium and paroxysmal supraventricular

tachyarrhythmia. Eur Heart J. 1988;9:1112-8. doi: 10.1093/oxfordjournals.eurheartj.a062407]

8. Bayes de Luna A, Oter MC, Guindo J. Interatrial conduction block with retrograde activation of the left atrium and paroxysmal supraventricular tachyarrhythmias: influence of preventive antiarrhythmic treatment. Int J Cardiol. 1989;22:147-50.

9. Bayes de Luna A, Fort de Ribot R, Trilla E, *et al.* Electrocardiographic and vectorcardiographic study of interatrial conduction disturbances with left atrial retrograde activation. J Electrocardiol. 1985;18:1-13.

10. Bayés de Luna A. The ECG for beginners. USA: Wiley-Blackwell; 2014.

11. Bayés de Luna A, Gusí Gené C, Soler Soler J, *et al.* Electrocardiologia clínica (2 volúmenes). Barcelona, Spain: Cinetiífico-Médica; 1977.

12. Bayes de Luna A, Platonov P, Cosio FG, *et al.* Interatrial blocks. A separate entity from left atrial enlargement: a consensus report. J Electrocardiol. 2012;45:445-51. doi: 10.1016/j.jelectrocard.2012.06.029]

13. Baranchuk A, Bayes-Genis A. Bayes' Syndrome. Rev Esp Cardiol (Engl Ed). 2016;69:439. doi: 10.1016/j.rec.2015.12.013]

14. Ariyarajah V, Spodick DH. Advanced interatrial block: a classic electrocardiogram. Cardiology. 2005;104:33-4. doi: 10.1159/000086052]

15. Waldo AL, Vitikainen KJ, Hoffman BF. The sequence of retrograde atrial activation in the canine heart. Correlation with positive and negative retrograde P waves. Circ Res. 1975;37:156-63. doi: 10.1161/01.res.37.2.156]

16. Spodick DH, Ariyarajah V, Apiyasawat S. Higher prevalence of cardiovascular events among patients with abnormal atrial depolarization and coronary artery disease at 18 months' post-exercise tolerance testing. Am Heart Hosp J. 2007;5:236-40.

17. Miquel C, Sodi-Pallares D, Cisneros F, *et al.* Right bundle branch block and right ventricular hypertrophy; electrocardiographic and vectorcardiographic diagnosis. Am J Cardiol. 1958;1:57-67. doi: 10.1016/0002-9149(58)90076-6]

18. Bussink BE, Holst AG, Jespersen L, *et al.* Right bundle branch block: prevalence, risk factors, and outcome in the general population: results from the Copenhagen City Heart Study. Eur Heart J. 2013;34:138-46. doi: 10.1093/eurheartj/ehs291]

19. de Micheli A, Medrano GA, Martinez Rios MA. [Right blocks in interauricular communication]. Arch Inst Cardiol Mex. 1978;48:1091-113.

20. Tabatabaei N, Katanyuwong P, Breen JF, *et al.* Images in cardiovascular medicine. Uncommon variant of Ebstein anomaly with tricuspid stenosis. Circulation. 2009;120:e1-2. doi: 10.1161/CIRCULATIONAHA.108.835652]

21. Hebert JL, Duthoit G, Hidden-Lucet F, *et al.* Images in cardiovascular medicine. Fortuitous discovery of partial Uhl anomaly in a male adult. Circulation. 2010;121:e426-9. doi: 10.1161/CIRCULATIONAHA.110.960773]

22. Gelband H, Waldo AL, Kaiser GA, *et al.* Etiology of right bundle-branch block in patients undergoing total correction of tetralogy of Fallot. Circulation. 1971;44:1022-33. doi: 10.1161/01.cir.44.6.1022]

23. Krongrad E, Hefler SE, Bowman FO, Jr., *et al.* Further observations on the etiology of the right bundle branch block pattern following right ventriculotomy. Circulation. 1974;50:1105-13. doi: 10.1161/01.cir.50.6.1105]

24. Riera AR, de Cano SJ, Cano MN, *et al.* Vector electrocardiographic alterations after percutaneous septal ablation in obstructive hypertrophic cardiomyopathy. Possible anatomic causes. Arq Bras Cardiol. 2002;79:466-75. doi: 10.1590/s0066-782x2002001400004]

25. Tomita M, Kitazawa H, Sato M, *et al.* A complete right bundle-branch block masking Brugada syndrome. J Electrocardiol. 2012;45:780-2. [PMID: 3483429 doi: 10.1016/j.jelectrocard.2012.06.019]

26. Zamfirescu NR, Ciplea A, Filcescu V, *et al.* [Right branch block associated with anterior left hemiblock; electrocardiographic and vectorcardiographic aspects]. Physiologie. 1978;15:269-78.

27. Retamal E, Illanes A, Moreno J. [Vectorcardiographic study of 15 patients with anterior left hemiblock and right branch block]. Rev Med Chil. 1972;100:1077-81.

28. Medrano GA, Brenes C, De Micheli A, *et al.* [Block of the anterior subdivision of the left bundle-branch, isolated or combined with right bundle-branch block. Clinical, electro and vectorcardiography studies]. Arch Inst Cardiol Mex. 1969;39:672-87.

29. Cergueira-Gomes M, Correia-dos-Santos J, Paula-Pinto R, *et al.* Right bundle branch block combined with left axis deviation: a vectorcardiographic study of 48 cases. J Electrocardiol. 1972;5:127-34.

30. Lichstein E, Chadda KD, Gupta PK. Complete right bundle branch block with left axis deviations: significance of vectorcardiographic morphology. Am Heart J. 1973;86:13-22. doi: 10.1016/0002-8703(73)90004-5]

31. Dubner S, Schapachnik E, Riera AR, *et al.* Chagas disease: state-of-the-art of diagnosis and management. Cardiol J. 2008;15:493-504.

32. Ribeiro AL, Marcolino MS, Prineas RJ, *et al.* Electrocardiographic abnormalities in elderly Chagas disease patients: 10-year follow-up of the Bambui Cohort Study of Aging. J Am Heart Assoc. 2014;3:e000632. [PMID: 3959704 doi: 10.1161/JAHA.113.000632]

33. Villongco CT, Krummen DE, Stark P, *et al.* Patient-specific modeling of ventricular activation pattern using surface ECG-derived vectorcardiogram in bundle

branch block. Prog Biophys Mol Biol. 2014;115:305-13. [PMID: 4254140 doi: 10.1016/j.pbiomolbio.2014.06.011]

34. Rodriguez-Padial L, Rodriguez-Picon B, Jerez-Valero M, *et al.* Diagnostic accuracy of computer-assisted electrocardiography in the diagnosis of left ventricular hypertrophy in left bundle branch block. Rev Esp Cardiol (Engl Ed). 2012;65:38-46. doi: 10.1016/j.recesp.2011.07.018]

35. Liakopoulos V, Kellerth T, Christensen K. Left bundle branch block and suspected myocardial infarction: does chronicity of the branch block matter? Eur Heart J Acute Cardiovasc Care. 2013;2:182-9. [PMID: 3821807 doi: 10.1177/2048872613483589]

36. Brembilla-Perrot B, Alla F, Suty-Selton C, *et al.* Nonischemic dilated cardiomyopathy: results of noninvasive and invasive evaluation in 310 patients and clinical significance of bundle branch block. Pacing Clin Electrophysiol. 2008;31:1383-90. doi: 10.1111/j.1540-8159.2008.01199.x]

37. Chan DD, Wu KC, Loring Z, *et al.* Comparison of the relation between left ventricular anatomy and QRS duration in patients with cardiomyopathy with versus without left bundle branch block. Am J Cardiol. 2014;113:1717-22. [PMID: 4051227 doi: 10.1016/j.amjcard.2014.02.026]

38. Poels TT, Houthuizen P, Van Garsse LA, *et al.* Transcatheter aortic valve implantation-induced left bundle branch block: causes and consequences. J Cardiovasc Transl Res. 2014;7:395-405. doi: 10.1007/s12265-014-9560-x]

39. Silva JA, Khuri B, Barbee W, *et al.* Systolic excursion of the mitral annulus to assess septal function in paradoxic septal motion. Am Heart J. 1996;131:138-45. doi: 10.1016/s0002-8703(96)90062-9]

40. Bharati S, Lev M, Dhingra RC, *et al.* Electrophysiologic and pathologic correlations in two cases of chronic second degree atrioventricular block with left bundle branch block. Circulation. 1975;52:221-9. doi: 10.1161/01.cir.52.2.221]

41. Kyndt F, Probst V, Potet F, *et al.* Novel SCN5A mutation leading either to isolated cardiac conduction defect or Brugada syndrome in a large French family. Circulation. 2001;104:3081-6. doi: 10.1161/hc5001.100834]

42. Asatryan B, Medeiros-Domingo A. Molecular and genetic insights into progressive cardiac conduction disease. Europace. 2019. doi: 10.1093/europace/euz109]

43. Mavrogeni S, Karabela G, Stavropoulos E, *et al.* Heart failure imaging patterns in systemic lupus erythematosus. Evaluation using cardiovascular magnetic resonance. Int J Cardiol. 2014;176:559-61. doi: 10.1016/j.ijcard.2014.07.016]

44. Rowinsky EK, McGuire WP, Guarnieri T, *et al.* Cardiac disturbances during the administration of taxol. J Clin Oncol. 1991;9:1704-12. doi: 10.1200/JCO.1991.9.9.1704]

45. Bellavia D, Pellikka PA, Abraham TP, *et al.* 'Hypersynchronisation' by tissue velocity imaging in patients with cardiac amyloidosis. Heart. 2009;95:234-40. doi: 10.1136/hrt.2007.140343]

46. Strauss DG, Selvester RH, Wagner GS. Defining left bundle branch block in the era of cardiac resynchronization therapy. Am J Cardiol. 2011;107:927-34. doi: 10.1016/j.amjcard.2010.11.010]

47. Manohar N, Young ML. Rate dependent bundle branch block induced by hyperkalemia. Pacing Clin Electrophysiol. 2003;26:1909-10. doi: 10.1046/j.1460-9592.2003.00291.x]

48. Al-Hadi H, Sallam M. Asymptomatic Permanent Left Bundle Branch Block (LBBB) complicating Diagnostic Left Heart Catheterisation. Sultan Qaboos Univ Med J. 2010;10:114-9. [PMID: 3074665

49. Castellanos A, Jr., Chapunoff E, Castillo CA, *et al.* The vectorcardiogram in left posterior hemiblock associated with inferior wall myocardial infarction. Chest. 1972;61:221-7. doi: 10.1378/chest.61.3.221]

50. Perez-Riera AR, Barbosa-Barros R, Daminello-Raimundo R, *et al.* The tetrafascicular nature of the intraventricular conduction system. Clin Cardiol. 2019;42:169-74. doi: 10.1002/clc.23093]

51. Damjanovic MR, Dordevic-Radojkovic D, Perisic Z, *et al.* [Ebstein's anomaly as a cause of paroxysmal atrial fibrillation]. Vojnosanit Pregl. 2008;65:847-50.